



Cite this: *Org. Biomol. Chem.*, 2018, **16**, 6801

Received 6th August 2018,
Accepted 3rd September 2018

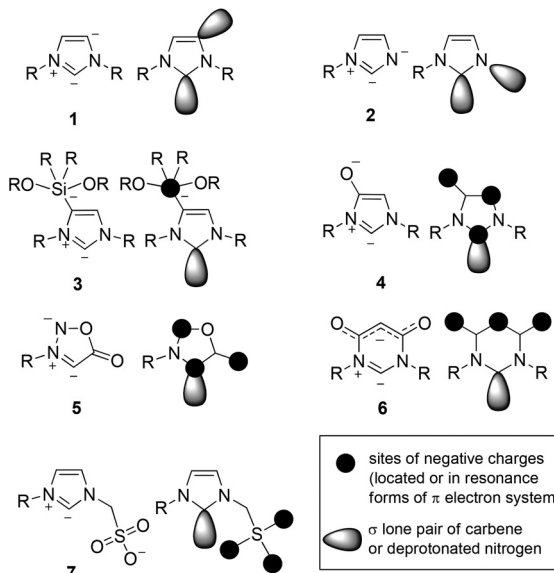
DOI: 10.1039/c8ob01916a

rsc.li/obc

Introduction

Anionic N-heterocyclic carbenes are interesting target molecules, because their σ -donicities as well as their π -electron characteristics can be adjusted by their molecular architecture in combination with their type of conjugation. Structures, syntheses and applications of first anionic N-heterocyclic carbenes have been summarized in a review article¹ and some publications appeared since then.² A closer look at the hitherto described examples reveals that the term “anionic N-heterocyclic carbene” encompasses fundamentally different types of structures. Thus, the first anionic N-heterocyclic dicarbene **1** (Scheme 1), containing both normal (C2) and abnormal carbene (C4) partial structures, was prepared by lithiation of the corresponding imidazole-2-ylidene and was obtained as the polymer $[\text{C}\{(\text{N}(2,6\text{-iPr}_2\text{C}_6\text{H}_3)]_2\text{CHClLi}(\text{THF})\}]_n$.³ Reviews summarizing the chemical properties of carbenes of this type⁴ and results of studies on coordination of metals in general⁵ as well as main group elements have been published.⁶ Neither the negative charge of the anionic N-heterocyclic carbene **1** nor that of anion **2**⁷ are delocalized in terms of resonance. In

contrast to the abnormal carbene structure of **1**, the anionic NHC **2** possesses a deprotonated nitrogen atom of a N3-unsubstituted imidazole. The anionic N-heterocyclic carbene **3** is substituted by a siliconate group at C4⁸ and the corresponding boron derivatives belong to a similar molecular architecture.⁹ The anions **4**¹⁰ and **5**¹¹ were prepared by deprotonation of



Scheme 1

^aClausthal University of Technology, Institute of Organic Chemistry, Leibnizstrasse 6, D-38678 Clausthal-Zellerfeld, Germany. E-mail: schmidt@ioc.tu-clausthal.de

^bUniversity of Helsinki, Department of Chemistry, Laboratory of Inorganic Chemistry, P.O. Box 55; FIN-00014 University of Helsinki, Finland

† Electronic supplementary information (ESI) available: Details of calculations. CCDC 1845098 (14). For ESI and crystallographic data in CIF or other electronic format see DOI: 10.1039/c8ob01916a

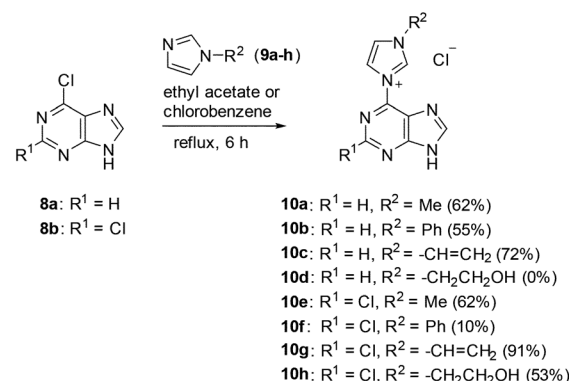


conjugated mesomeric betaines (CMB), *i.e.* imidazolium-olates and sydnone, respectively. As a consequence of their origin, the negative charge is delocalized within the π -conjugated system which sets them apart from the anionic N-heterocyclic carbenes **1**, **2**, and **3**. The canonical formulae of **4** and **5** identify the carbene carbon atoms as sites of the negative charges. Consequently the carbene carbon atoms display considerable atomic orbital coefficients of the calculated highest occupied molecular orbitals (HOMO or HOMO-1) which are π -orbitals, respectively. Thus, the π -electron donor/acceptor properties of the NHCs can be influenced by the architecture of the molecules. With respect to this, the pyrimidine derivative **6** clearly belongs to another type of anionic N-heterocyclic carbene, because it was generated from a cross-conjugated mesomeric betaine (CCMB). Consequently the negative charge is exclusively delocalized in the 3-oxobut-1-en-1-olate partial structure according to the resonance forms without mesomeric charge distribution into the diaminocarbene moiety.¹² No conjugation at all between the anionic substituent and the N-heterocyclic carbene moiety of **7** exists, as this anionic N-heterocyclic carbene was prepared by deprotonation of a zwitterionic starting material with isolated anionic and positive charges.¹³ Thus, carbene **7** is an example of a type of anionic N-heterocyclic carbene which differs from all aforementioned molecules. The chemistry of N-heterocyclic carbenes in the light of history¹⁴ as well as the intersection between the substance classes of mesomeric betaines and N-heterocyclic carbenes have been reviewed.¹⁵

In continuation of our interest in mesomeric betaines¹⁶ and their conversion into N-heterocyclic carbenes,^{14,15} and as part of our studies directed toward the chemical and physical consequences of different types of conjugation, we describe here imidazol-2-ylidene which are in π -conjugation with an anionic purinate which serves as π -electron donator *via* N1 of the imidazole.

Results and discussion

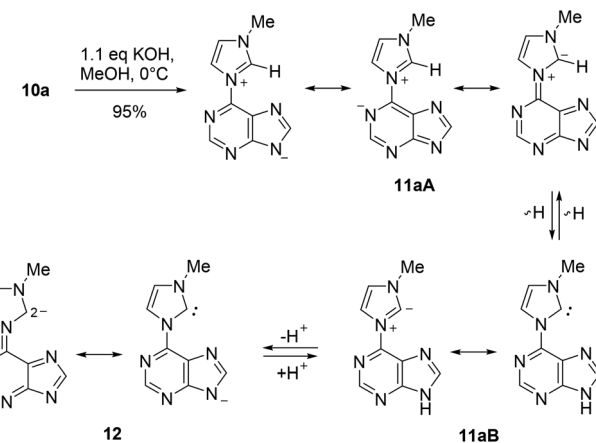
A series of purin-6-yl-imidazolium chlorides was prepared starting from substituted imidazoles, 6-chloropurine **8a** and 2,6-dichloropurine **8b**, respectively (Scheme 2). The reaction of **8a** required chlorobenzene as solvent, whereas reactions of **8b** proceeded best in ethyl acetate. The salts **10a-h**, except for **10d**, were obtained in medium to excellent yields as colourless solids under these conditions, respectively. The ^1H NMR signals of the H/D exchangeable 2-*H*_{imidazolium} appear between 10.39 ppm and 10.99 ppm. We tried a series of bases to deprotonate the salts **10**. The anion exchange resins Amberlite IRA-400 and IRA-96 in their hydroxide forms, respectively, proved to be unsuited reagents to deprotonate the salts, because the resulting mesomeric betaines or their tautomeric N-heterocyclic carbenes were bound on the resins and could not be eluted. The system consisting of silica gel, ethyl acetate, and petroleum ether with small amounts of triethylamine proved to be a suited medium to deprotonate the salts to the



Scheme 2

corresponding mesomeric betaines under mild conditions. However, the mesomeric betaines proved to be unstable on trying to remove the solvents or on storage in solution. An exception is the mesomeric betaine **11a** which is remarkably stable. It was best obtained in 95% yield on deprotonation with potassium hydroxide in methanol under cooling with ice (Scheme 3).

On betaine formation, considerable chemical shift changes of the purinyl substituent can be observed. Thus, $\Delta\delta_{2-H}$ and $\Delta\delta_{8-H}$ of the purine moiety are shifted by 0.44 ppm and 0.69 ppm to higher field, respectively. The signal of 2-*H* of the imidazolium ring appears at δ = 10.37 ppm in DMSO-d₆ so that exclusively tautomer **11aA** seems to be present under these conditions. No traces of the N-heterocyclic carbene tautomer **11aB** was detected and this observation is in analogy to imidazolium-phenolates,¹⁷ imidazolium-isocytosinates,¹⁸ imidazolium-indolates,¹⁹ imidazolium-azaindolates,¹⁹ triazolium-indolates,¹⁹ and nitrone.²⁰ Deprotonation of the mesomeric betaine **11a** resulted in the formation of an anionic N-heterocyclic carbene **12** which was clearly detected as the base peak at *m/z* = 201.0885 (calcd 201.0883) in high resolution electrospray ionization mass spectrometry. In accordance with the rules of resonance two negative charges can be formulated



Scheme 3



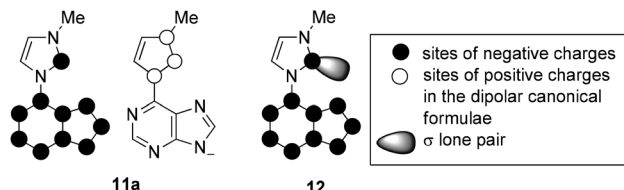


Fig. 1 Charge distribution according to the resonance forms.

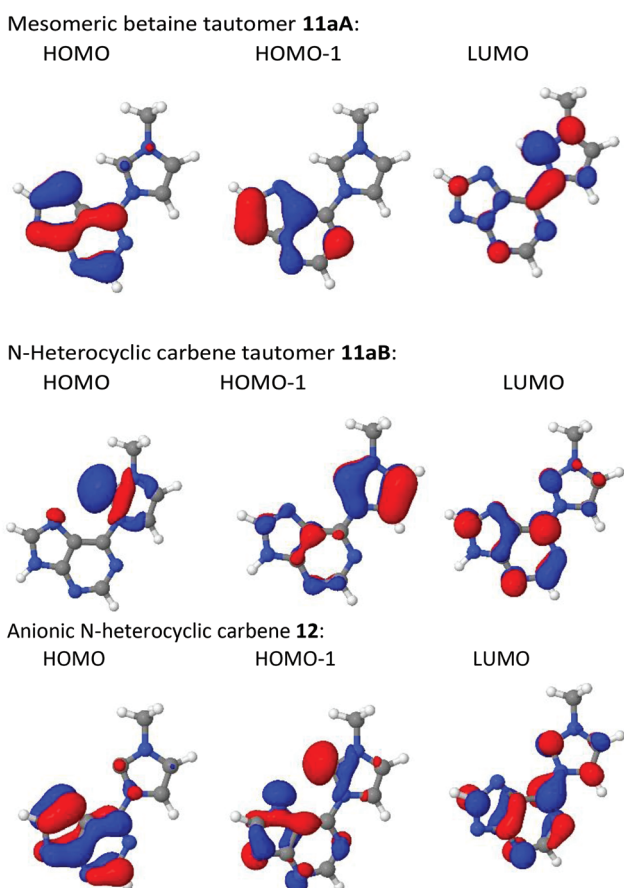
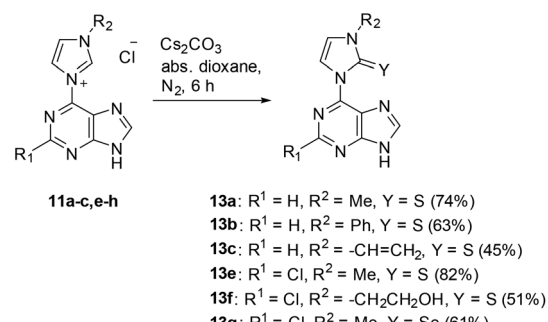
at C2 of the imidazole moiety, one of which is caused by the pair of electrons in the sp^2 hybrid orbital in the plane of the heteroaromatic ring and the other one is due to the delocalization within the common π -electron system.

The sites of negative charges and positive charges in the canonical formulae of the mesomeric betaine **11a** are shown in Fig. 1. As C2 of the imidazolium ring is a site of either charge, this mesomeric betaine can unambiguously be classified as a conjugated system (CMB).²¹ The carbene carbon atom C2 of the anionic N-heterocyclic carbene **12** remains a site of negative charge in the resonance forms.

According to DFT calculations the highest occupied molecular orbital (HOMO) of the mesomeric betaine tautomer **11aA** is essentially located in the purine ring, and the same is true for the HOMO-1 (Fig. 2). By contrast, the LUMO is distributed

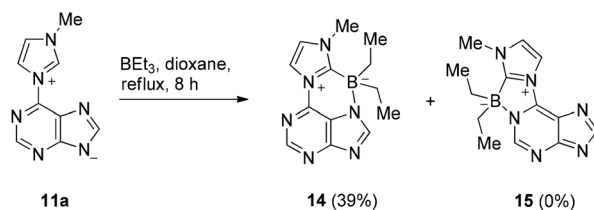
over the entire π -electron system. A large coefficient of the LUMO is located on the bond which connects the purine ring with the imidazole ring which has a calculated bond length of 1.43 Å. The betaine was calculated to be almost perfectly planar ($\tau = 0.031^\circ$). The HOMO of the corresponding N-heterocyclic carbene tautomer **11aB** is a σ lone pair located at the carbene carbon atom, whereas the HOMO-1's atomic orbital coefficients are essentially located in the π -electronic system of the imidazole ring with smaller contributions in the purine's π -electron system. The LUMO, by contrast, possesses its major coefficients in the purine ring and on C2 of the imidazole ring. The bond length between the two ring systems was calculated to be slightly shortened (1.39 Å) in comparison to the mesomeric betaine tautomer, but the molecule remains planar on tautomerisation ($\tau = 0.59^\circ$). According to the calculation, the mesomeric betaine tautomer **11aA** is by approximately $dE = 53$ kJ mol⁻¹ (electronic energy) more stable *in vacuo* than the N-heterocyclic carbene tautomer **11aB**. As DMSO stabilizes more dipolar structures, the mesomeric betaine tautomer is even more stable in DMSO solution than in the vacuum (approximately $dE = 91$ kJ mol⁻¹). The anionic N-heterocyclic carbene **12** is not planar *in vacuo* according to the calculation. In contrast to the N-heterocyclic carbene tautomer **11aB** mentioned above, its HOMO is a π orbital which is located in the purine and the imidazole ring including contributions at C2_{imidazol-2-ylidene}. By contrast, the HOMO-1 is a σ lone pair at the carbene carbon atom plus considerable atomic orbital coefficients especially in the five-membered fragment of the purine ring. The coefficient at N₇_{purine} obviously causes the dihedral angle (19.9°) between the two ring systems by electronic repulsion to the σ lone pair at C2_{imidazole}. The torsion, however, is small enough to allow conjugation between the two rings. The LUMO of the N-heterocyclic carbene is distributed all over the π -electron system. The bond length between the two ring systems was calculated to be 1.42 Å.

When the purine salts are treated with elemental sulphur and selenium in the presence of bases, respectively, they behave as N-heterocyclic carbenes and yield imidazole-thiones and imidazole-selenones in acceptable yields (Scheme 4).

Fig. 2 Frontier orbitals of **11aA**, **11aB**, and **12**.

Scheme 4





Scheme 5

The anionic N-heterocyclic carbene can formally be trapped as boron adduct. Thus, reaction of the mesomeric betaine **11a** with triethylborane at $140\text{ }^\circ\text{C}$ in anhydrous dioxane in an autoclave resulted in the formation of the first representative of a new heterocyclic ring system, imidazo[2',1':3,4][1,4,2] diazaborino[1,6-5,gh]purinium-7-ide **14** (Scheme 5).

To exclude the formation of its regiosomer **15**, a combination of H,H -COSY-, H,C -HSQC-, H,C -HMBC-, and NOESY-experiments was carried out. NOESY correlations between $\text{C}_{8\text{purine}}$ and the ethyl groups attached to the boron atom proved the formation of the regiosomer **14** possessing the six-membered ring with a bond between $\text{N}_{7\text{purine}}$ and the boron atom (Fig. 3).

Single crystals of the boron adduct **14** were obtained by slow evaporation of a concentrated solution in ethyl acetate. The boron adduct crystallized triclinic (Fig. 4). The torsion angle between imidazole and the purine ring [C7A-C7-N8-C12 , crystallographic numbering] was determined to be $-1.76(15)^\circ$. The dihedral angles C12-B1-N1-C7A and N1-B1-C12-N8 were found to be $-17.39(12)^\circ$ and $19.10(14)^\circ$, respectively. The bond length between the boron atom and the former carbene carbon atom is $1.6643(16)$ Å, whereas the bond between the boron atom and the methylene carbon atoms of the ethyl groups was found to have a bond length of $1.6226(16)$ Å and $1.6315(17)$ Å. The bond distance between the boron atom and the nitrogen atom is $1.6003(14)$ Å.

According to a DFT calculation, the HOMO of the boron adduct consists of π orbital contributions of the purine ring plus the B-C σ bonds between the boron atom and the methylene moiety of the ethyl groups (Fig. 5). The LUMO is distributed all over the π electron system. The angles C7-N8-C12-B1 and B1-N1-C7A-C7 were determined to be $-10.66(16)$ and $9.97(18)$, respectively.

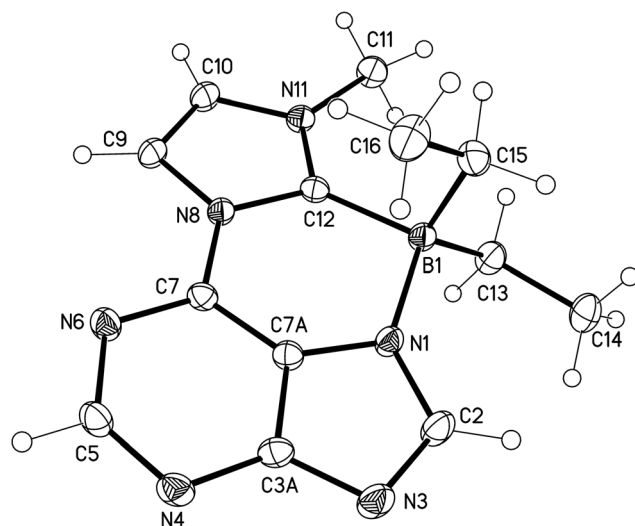


Fig. 4 Molecular drawing of the boron adduct **14** of the anionic N-heterocyclic carbene **12** (displacement parameters are drawn at 50% probability level).

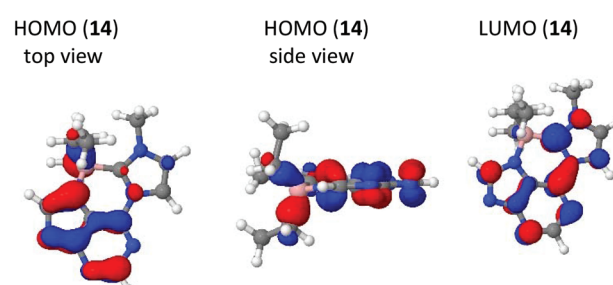


Fig. 5 Frontier orbitals of **14**.

Experimental

The reactions were carried out under an atmosphere of nitrogen in oven-dried glassware. Nuclear magnetic resonance (NMR) spectra were obtained with a Bruker Avance 400 and Bruker Avance III 600 MHz. ^1H NMR spectra were measured at 400 MHz or 600 MHz and ^{13}C NMR spectra were measured at 100 MHz or 150 MHz, with the solvent peak or tetramethylsilane used as the internal reference. Multiplicities are described by using the following abbreviations: s = singlet, d = doublet, t = triplet, q = quartet, and m = multiplet, and the signal orientations in DEPT experiments were described as follows: o = no signal; + = up (CH , CH_3); - = down (CH_2). ATR-IR spectra were obtained on a Bruker Alpha in the range of 400 to 4000 cm^{-1} . The mass spectra were measured with a Varian 320 MS Triple Quad GC/MS/MS with a Varian 450-GC. The electrospray ionization mass spectra (ESIMS) were measured with an Agilent LCMSD series HP 1100 with APIES. The compound samples were sprayed from MeCN at 4000 V capillary voltage and fragmentor voltages of 30 V, unless otherwise noted. The HR-MS spectra were obtained with a Bruker

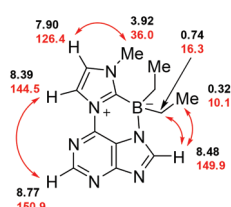


Fig. 3 Diagnostic NOESY correlations. Values of ^1H NMR shifts (in black) and ^{13}C NMR shifts (in red) [ppm], respectively.



Impact II or a Bruker Daltonik Tesla-Fourier transform-ion cyclotron resonance mass spectrometer with electrospray ionization or a Waters Micromass LCT with direct inlet. Melting points are uncorrected and were determined in an apparatus according to Dr Tottoli (Büchi). Yields are not optimized.

Calculations

All density-functional theory (DFT)-calculations were carried out by using the Firefly 8.2.0 QC package,²² which is partially based on the GAMESS (US)²³ source code, running on Linux 2.6.18-238.el5 SMP (x86_64) on five AMD Phenom II X6 1090T processor workstations (Beowulf-cluster) with Infiniband interconnect and parallelized with MPICH 1.2.7p1. MM2 optimized structures were used as starting geometries. Complete geometry optimizations were carried out on the implemented N31G6* basis set and with the PBE0 density functional. All calculated structures were proven to be true minima by the absence of imaginary frequencies. Solvent effects were estimated by help of the polarizable continuum model (PCM) implemented in Firefly. Partial charges were obtained with NBO 5.9²⁴ from the results of the DFT calculations. Orbital plots were obtained using Jmol 14.27.2.

Crystal structure determination of 14

The single-crystal X-ray diffraction study was carried out on a Bruker D8 Venture diffractometer with Photon100 detector at 123(2) K using Cu-K α radiation ($\lambda = 1.54178$ Å). Direct Methods (SHELXS-97)²⁵ were used for structure solution and refinement was carried out using SHELXL-2014 (full-matrix least-squares on F^2).²⁶ Hydrogen atoms were localized by difference electron density determination and refined using a riding model. A semi-empirical absorption correction and an extinction correction were applied.

14: colourless crystals, $C_{13}H_{17}BN_6$, $M_r = 268.13$, crystal size $0.36 \times 0.36 \times 0.12$ mm, triclinic, space group $P\bar{1}$ (no. 2), $a = 7.2834(4)$ Å, $b = 7.5733(4)$ Å, $c = 12.2004(7)$ Å, $\alpha = 92.486(2)^\circ$, $\beta = 94.926(2)^\circ$, $\gamma = 96.678(2)^\circ$, $V = 664.96(6)$ Å 3 , $Z = 2$, $\rho = 1.339$ Mg m $^{-3}$, $\mu(\text{Cu-K}\alpha) = 0.680$ mm $^{-1}$, $F(000) = 284$, $2\theta_{\text{max}} = 144.4^\circ$, 10 331 reflections, of which 2589 were independent ($R_{\text{int}} = 0.022$), 183 parameters, $R_1 = 0.036$ (for 2467 $I > 2\sigma(I)$), $wR_2 = 0.095$ (all data), $S = 1.04$, largest diff. peak/hole = $0.300/-0.178$ e Å $^{-3}$.

CCDC 1845098 (**14**)† contains the supplementary crystallographic data for this paper.

1-Methyl-3-(9H-purin-6-yl)-1H-imidazolium chloride 10a

Samples of 618 mg (4.0 mmol) of 6-chloropurine and 984 mg (12.0 mmol) of 1-methylimidazole were dissolved in 20 mL of chlorobenzene. Then, the solution was heated under reflux over a period of 7 h. After cooling to rt, the resulting precipitate was filtered off, washed with diethylether and recrystallized from ethyl acetate. Yield: 584 mg (62%) of a colourless solid, dec. 358 °C (from EtOAc). $\nu_{\text{max}}/\text{cm}^{-1} = 2241, 3235, 3122, 3086, 1615, 1573, 1533, 1441, 1346, 1293, 1184, 1129, 1106, 916, 841, 767, 646, 573, 534, 406$. δH (400 MHz; DMSO-d₆)

10.39 (s, 1H), 8.99 (s, 1H), 8.92 (s, 1H), 8.84 (m, 1H), 8.06 (m, 1H), 4.09 (s, 3H) ppm. δC (100 MHz; DMSO-d₆) 155.6, 151.4, 147.4, 141.7, 137.2, 125.0, 122.0, 119.8, 36.6 ppm. m/z (ESIMS) 201.1 (M) $^+$. HR-ESI-MS [C₉H₉N₆]: calcd 201.0883 [M] $^+$, found 201.0886.

1-Phenyl-3-(9H-purin-6-yl)-1H-imidazolium chloride 10b

Synthesis in analogy to 10a. 1152 mg (8.0 mmol) of 1-phenylimidazole were used. Yield: 657 mg (55%) of a dark solid, dec. 288 °C (from EtOAc). $\nu_{\text{max}}/\text{cm}^{-1} = 3141, 2998, 1623, 1530, 1456, 1401, 1328, 1259, 1113, 1064, 914, 841, 774, 766, 693, 638, 606, 518, 451$. δH (400 MHz; DMSO-d₆) 10.78 (m, 1H), 9.12 (dd, $J = 2.2/1.8$ Hz, 1H), 9.05 (s, 1H), 8.95 (s, 1H), 8.65 (dd, $J = 2.2/1.8$ Hz, 1H), 8.00–7.98 (m, 2H), 7.74–7.67 (m, 3H) ppm. δC (100 MHz; DMSO-d₆) 151.5, 147.8, 141.5, 135.4, 134.5, 130.5, 130.2, 123.0, 122.7, 121.2 ppm. HR-ESI-MS [C₁₄H₁₁N₆]: calcd 263.1040 [M] $^+$. Found 263.1041.

1-Vinyl-3-(9H-purin-6-yl)-1H-imidazolium chloride 10c

Synthesis in analogy to 10a. 752 mg (8.0 mmol) of 1-vinylimidazole were used. Yield: 716 mg (72%) of a colourless solid, dec. 276 °C (from EtOAc). $\nu_{\text{max}}/\text{cm}^{-1} = 3063, 2855, 2612, 2520, 1618, 1568, 1538, 1464, 1329, 1222, 1140, 1113, 1035, 910, 760, 640, 605, 586, 547, 508$. δH (400 MHz; DMSO-d₆) 14.62 (s, 1H), 10.39 (s, 1H), 8.99 (s, 1H), 8.92 (s, 1H), 8.84 (m, 1H), 8.06 (m, 1H), 4.09 (s, 3H) ppm. δC (100 MHz; DMSO-d₆) 155.6, 151.4, 147.4, 141.7, 137.2, 125.0, 122.0, 119.8, 36.6 ppm. m/z (ESIMS) 213.1 (M) $^+$. HR-ESI-MS [C₁₀H₉N₆]: calcd 213.0883 [M] $^+$, found 213.0883.

(2-Chloro-9H-purin-6-yl)-1-methyl-1H-imidazolium chloride 10e

A sample of 189 mg (1.0 mmol) of 2,6-dichloropurine and 164 mg (2.0 mmol) of 1-methylimidazol were dissolved in 10 mL of ethyl acetate and heated under reflux for 7 h. After cooling to rt the resulting precipitate was filtered off, washed with diethylether and recrystallized from ethyl acetate. Yield: 168 mg (62%) of a colourless solid, dec. 367 °C (from EtOAc). $\nu_{\text{max}}/\text{cm}^{-1} = 3057, 2636, 1694, 1586, 1331, 1178, 1015, 859, 839, 791, 634, 617, 598, 547$. δH (400 MHz; D₂O) 8.63 (s, 1H), 8.62 (d, $J = 2.2$ Hz, 1H), 7.81 (d, $J = 2.2$ Hz, 1H), 4.15 (s, 3H) ppm. δC (100 MHz; D₂O) 160.1, 155.4, 151.2, 145.3, 140.1, 127.8, 124.7, 123.1, 39.8 ppm. m/z (ESIMS) 235.0 (M) $^+$. HR-ESI-MS [C₉H₈N₆]: calcd 235.0499 [M] $^+$, found 235.0498.

1-Phenyl-3-(2-chloro-9H-purin-6-yl)-1H-imidazolium chloride 10f

Synthesis in analogy to 10e. 288 mg (2.0 mmol) of 1-phenyl-1H-imidazole were used. Yield: 33 mg (10%) of a colourless oil. δH (400 MHz; DMSO-d₆) 10.77 (s, 1H), 9.07 (d, $J = 2.2$ Hz, 1H), 9.00 (s, 1H), 8.68 (d, $J = 2.2$ Hz, 1H), 8.02–8.00 (m, 2H), 7.73–7.67 (m, 3H) ppm. δC (100 MHz; DMSO-d₆) 151.2, 148.6, 142.1, 135.6, 134.3, 130.5, 130.1, 129.0, 123.1, 122.8, 121.8, 121.3 ppm. Compound proved to be unstable.

3-(2-Chloro-9H-purin-6-yl)-1-vinyl-1H-imidazolium chloride 10g

Synthesis in analogy to 10e. 188 mg (2.0 mmol) of 1-vinylimidazole were used. Yield: 258 mg (91%) of a colourless solid,



dec. 282 °C (from EtOAc). $\nu_{\text{max}}/\text{cm}^{-1}$ 3073, 3046, 2625, 2504, 1620, 1567, 1538, 1335, 1232, 1180, 1112, 921, 761, 629, 590. δH (400 MHz; D₂O) 8.75 (d, J = 2.3 Hz, 1H), 8.67 (s, 1H), 8.17 (d, J = 2.3 Hz, 1H), 7.40 (dd, J = 15.5/8.6 Hz 1H), 6.11 (dd, J = 15.5/3.1 Hz, 1H), 5.70 (dd, J = 8.6/3.1 Hz, 1H) ppm. δC (100 MHz, D₂O) 160.5, 155.1, 151.7, 145.2, 131.0, 124.9, 123.8, 123.7, 115.2 ppm. m/z (ESIMS) 247.0 [M]⁺. HR-ESI-MS [C₁₀H₈N₆]: calcd 247.0499 [M]⁺, found 247.0499.

3-(2-Chloro-9H-purin-6-yl)-1-(2-hydroxyethyl)-1H-imidazolium chloride 10h

Synthesis in analogy to 10e. 316 mg (2.0 mmol) of 1-hydroxyethylimidazole were used. Yield: 184 mg (53%) of a colourless solid, dec. 321 °C (from EtOAc). $\nu_{\text{max}}/\text{cm}^{-1}$: 3266, 3073, 2880, 2746, 1619, 1574, 1540, 1326, 1249, 1171, 1137, 1063, 1038, 845, 789, 750, 629, 578, 547, 496. δH (400 MHz; DMSO-d₆) 10.84 (s, 1H), 8.83 (s, 1H), 8.82 (m, 1H), 8.11 (m, 1H), 4.50 (t, J = 5.0 Hz, 2H), 3.84 (t, J = 5.0 Hz, 2H) ppm. δC (100 MHz; DMSO-d₆) 159.5, 150.6, 150.3, 141.6, 136.9, 124.4, 122.1, 120.0, 59.8, 52.4 ppm. m/z (ESIMS) 265.0 [M]⁺. HR-ESI-MS [C₁₀H₁₀N₆O]: calcd 265.0605 [M]⁺, found 265.0606.

6-(1-Methyl-1H-imidazolium-3-yl)purin-7-ide 11a

A sample of 237 mg (1.0 mmol) of the salt **10a** was suspended in 50 mL of anhyd methanol and cooled to 0 °C. Then, 50 mL of KOH in water (1.1 mol L⁻¹) was added dropwise. After 30 minutes of stirring at that temperature, the suspension was evaporated to dryness. The crude product was washed with ice-cold water and dried *in vacuo*. Yield: 190 mg (95%) of a colourless solid, dec. 308 °C (from H₂O). $\nu_{\text{max}}/\text{cm}^{-1}$ 3306, 3160, 2109, 3086, 1657, 1612, 1575, 1533, 1441, 1345, 1293, 1240, 1184, 1105, 1089, 915, 841, 766, 645, 572, 534, 406. δH (400 MHz; D₂O) 10.37 (s, 1H), 8.87 (m, 1H), 8.55 (s, 1H), 8.23 (s, 1H), 7.94 (m, 1H), 4.04 (s, 3H) ppm. δC (100 MHz; D₂O) 167.6, 159.8, 146.4, 137.7, 136.3, 124.4, 124.2, 119.4, 36.3 ppm. m/z (ESIMS) 201.1 [M + H]⁺. HR-ESI-MS [C₉H₈N₆]: calcd 201.0883 [M + H]⁺, found 201.0885.

1-Methyl-3-(9H-purin-6-yl)-1,3-dihydro-2H-imidazole-2-thione 13a

A suspension of 326 mg (1.0 mmol) of caesium carbonate, 109 mg (0.5 mmol) of salt **10a**, and 22 mg (0.7 mmol) of sulfur in 15 mL of anhyd acetonitrile was heated under nitrogen over a period of 7 h under reflux. After the solvent was distilled off *in vacuo*, the crude reaction product was chromatographed (silica gel, EtOAc). Yield: 86 mg (74%) of a yellow solid, dec. 258 °C (from EtOAc). $\nu_{\text{max}}/\text{cm}^{-1}$ 3108, 2922, 1623, 1554, 1460, 1446, 1383, 1368, 1351, 1249, 1179, 1100, 914, 844, 801, 732, 701, 666, 651, 612, 598, 547, 534. δH (400 MHz; DMSO-d₆) 8.93 (s, 1H), 8.69 (s, 1H), 7.47 (d, J = 2.5 Hz, 1H), 7.42 (d, J = 2.5 Hz, 1H), 3.58 (s, 3H) ppm. δC (100 MHz; DMSO-d₆) 162.7, 159.4, 151.3, 147.5, 144.4, 120.3, 117.4, 34.5 ppm. HR-ESI-MS for [C₉H₈N₆S]: calcd 255.0423 [M + Na]⁺. Found 255.0414.

1-Phenyl-3-(9H-purin-6-yl)-1,3-dihydro-2H-imidazole-2-thione 13b

Synthesis in analogy to 13a. 149 mg (0.5 mmol) of salt **10b** and 32 mg (1.0 mmol) of S₈ were used. Yield: 93 mg (63%) of a yellow solid, dec. 244 °C (from EtOAc). $\nu_{\text{max}}/\text{cm}^{-1}$ 3271, 3105, 1629, 1553, 1503, 1457, 1414, 1357, 1293, 845, 757, 689, 579, 552. δH (400 MHz; DMSO-d₆) 9.00 (s, 1H), 8.77 (s, 1H), 7.75 (m, 2H), 7.68 (d, J = 2.6 Hz, 1H), 7.66 (d, J = 2.6 Hz, 1H), 7.58 (m, 2H), 7.48 (m, 1H) ppm. δC (100 MHz; DMSO-d₆) 163.1, 151.5, 147.5, 137.7, 129.0, 128.2, 126.0, 120.2, 116.6 ppm. m/z (ESIMS) 317.0 [M + Na]⁺. HR-ESI-MS for [C₁₄H₁₀N₆S]: calcd 317.0580 [M + Na]⁺. Found 317.0586.

1-(9H-Purin-6-yl)-3-vinyl-1,3-dihydro-2H-imidazole-2-thione 13c

Synthesis in analogy to 13a. 124 mg (0.5 mmol) of **10c** were used. Yield: 55 mg (45%) of a yellow solid, dec. 262 °C (from EtOAc). $\nu_{\text{max}}/\text{cm}^{-1}$ 2147, 3088, 1642, 1623, 1552, 1457, 1393, 1372, 1343, 1262, 1246, 1174, 1099, 913, 843, 712, 645, 592, 538. δH (400 MHz; DMSO-d₆) 8.98 (s, 1H), 8.74 (s, 1H), 7.90 (d, J = 2.1 Hz, 1H), 7.65 (d, J = 2.1 Hz, 1H), 7.50 (dd, J = 16.0/8.7 Hz, 1H), 5.65 (d, J = 16.0 Hz, 1H), 5.11 (d, J = 8.7 Hz, 1H) ppm. δC (100 MHz; DMSO-d₆) 162.7, 151.5, 147.5, 143.9, 129.0, 119.5, 114.9, 102.6 ppm. m/z (ESIMS) 267.0 [M + Na]⁺, 511.1 (2M + Na)⁺. HR-ESI-MS for [C₁₀H₈N₆S]: calcd 267.0423 [M + Na]⁺. Found 255.0428.

1-(2-Chloro-9H-purin-6-yl)-3-methyl-1,3-dihydro-2H-imidazole-2-thione 13e

Synthesis in analogy to 13a. 135 mg (0.5 mmol) of salt **10e** were used. Yield: 109 mg (82%) of an orange solid, dec. 264 °C (from EtOAc). $\nu_{\text{max}}/\text{cm}^{-1}$ 3277, 3177, 1635, 1545, 1413, 1382, 1223, 1199, 1094, 960, 930, 850, 672, 553, 537. δH (400 MHz; DMSO-d₆) 8.69 (s, 1H), 7.46 (d, J = 2.5 Hz, 1H), 7.42 (d, J = 2.5 Hz, 1H), 3.56 (s, 3H) ppm. δC (100 MHz; DMSO-d₆) 162.8, 162.7, 150.5, 150.4, 144.6, 120.5, 117.3, 34.5 ppm. m/z (ESIMS) 267.0 [M + H]⁺, 289.0 (M + Na)⁺, 555.0 (2M + Na)⁺. HR-ESI-MS for [C₉H₇N₆S]: calcd 267.0220 [M + H]⁺, found 267.0219.

1-(2-Chloro-9H-purin-6-yl)-3-(2-hydroxyethyl)-1,3-dihydro-2H-imidazole-2-thione 13f

Synthesis in analogy to 13a. 135 mg (0.5 mmol) of salt **10h** and 26 mg (0.8 mmol) of sulphur were used. Yield: 76 mg (51%), dec. 247 °C (from EtOAc). $\nu_{\text{max}}/\text{cm}^{-1}$ 3097, 2953, 1615, 1547, 1376, 1287, 1185, 1014, 932, 710, 603, 557. δH (400 MHz; DMSO-d₆) 8.67 (s, 1H), 7.44 (d, J = 2.6 Hz, 1H), 7.37 (d, J = 2.6 Hz, 1H), 4.10 (t, J = 5.6 Hz, 2H), 3.75 (t, J = 5.6 Hz, 2H) ppm. δC (100 MHz; DMSO-d₆) 162.3, 150.6, 150.3, 120.5, 117.1, 58.1, 49.5 ppm. m/z (ESIMS) 319.0 (M + Na)⁺, 615.0 (2M + Na)⁺. HR-ESI-MS for [C₁₀H₉N₆OS]: calcd 297.0325 [M + H]⁺, found 297.0324.

1-(2-Chloro-9H-purin-6-yl)-3-methyl-1,3-dihydro-2H-imidazole-2-selenone 13g

Synthesis in analogy to 13a. 135 mg (0.5 mmol) of salt **10e** and 79 mg (1.0 mmol) of selenium were used. Yield: 96 mg



(61%) of yellow solid, dec. 249 °C (from EtOAc). $\nu_{\text{max}}/\text{cm}^{-1}$ 3175, 3097, 1695, 1627, 1544, 1411, 1382, 1330, 1222, 1198, 1095, 929, 848, 790, 630, 571. δH (400 MHz; DMSO-d₆) 8.49 (s, 1H), 7.60 (d, J = 2.6 Hz, 1H), 7.57 (d, J = 2.6 Hz, 1H), 3.66 (s, 3H) ppm. δC (100 MHz; DMSO-d₆) 164.5, 156.3, 153.8, 149.1, 144.7, 128.2, 121.8, 120.2, 36.4 ppm. m/z (ESIMS) 313.0 (M - H)⁻. HR-ESI-MS [C₉H₇N₆Se]: calcd 336.9484 (M + Na)⁺, found 336.9485.

7,7-Diethyl-8-methyl-7,8-dihydroimidazo[2',1':3,4][1,4,2]diazaborinino[1,6,5-gh]purinium-7-ide 14

A solution of 242 mg (1.0 mmol) of triethylborane in 2 mL of anhyd dichloromethane was added dropwise into a suspension of 96 mg (0.5 mmol) of **11a** in 5 mL of the same solvent. The mixture was then heated to 200 °C under a nitrogen atmosphere for 24 h in a Schlenk tube. After cooling to rt, the solvent was distilled off *in vacuo* and the crude reaction product was chromatographed (silica gel, EtOH : EtOAc = 2 : 1). Yield: 91 mg (39%) of a colorless solid, dec. 314 °C (from EtOH/EtOAc). $\nu_{\text{max}}/\text{cm}^{-1}$ 2940, 2905, 2862, 2818, 1669, 1581, 1473, 1461, 1427, 1404, 1313, 1304, 1192, 1082, 1048, 847, 802, 641, 623, 571. δH (400 MHz; DMSO-d₆) 8.77 (s, 1H), 8.47 (s, 1H), 8.38 (d, J = 2.1 Hz, 1H), 7.90 (d, J = 2.1 Hz, 1H), 3.92 (s, 1H), 0.79–0.74 (m, 2H), 0.72–0.68 (m, 2H), 0.32 (t, J = 7.8 Hz, 6H) ppm. δC (100 MHz; DMSO-d₆) 161.7, 151.3, 150.3, 141.4, 126.7, 118.1, 114.8, 36.4, 16.7, 10.8 ppm. m/z (ESIMS) 269.1 (M + H)⁺, 559.3 (2M + Na)⁺. HR-ESI-MS for [C₁₃H₁₇BN₆] calcd 269.1681 (M + H)⁺. Found 269.1685.

Conclusions

(Purin-6-yl)-1-methyl-imidazolium salts can be deprotonated to give a stable mesomeric betaine, the N-heterocyclic tautomer of which can be trapped by sulphur and selenium. The corresponding anionic N-heterocyclic carbene formally gave a cyclic borane adduct which is the first representative of a new heterocyclic ring system, imidazo[2',1':3,4][1,4,2]diazaborinino[1,6,5-gh]purine.

Conflicts of interest

There are no conflicts to declare.

Acknowledgements

Dr Gerald Dräger, university of Hannover (Germany) is gratefully acknowledged for measuring a part of the HRMS spectra.

References

- 1 A. Nasr, A. Winkler and M. Tamm, *Coord. Chem. Rev.*, 2016, **316**, 68.

- 2 (a) H. Niu, R. J. Mangan, A. V. Protchenko, N. Phillips, W. Unkrig, C. Friedmann, E. L. Kolychev, R. Tirfoin, J. Hicks and S. Aldridge, *Dalton Trans.*, 2018, **47**, 7445; (b) J. B. Waters, L. S. Tucker and J. M. Goicoechea, *Organometallics*, 2018, **37**, 655; (c) A.-L. Lücke, S. Wiechmann, T. Freese, M. Nieger, T. Földes, I. Pápai, M. Gjikaj, A. Adam and A. Schmidt, *Tetrahedron*, 2018, **74**, 2092; (d) G. Kleinhans, G. Guisado-Barrios, E. Peris and D. I. Bezuidenhout, *Polyhedron*, 2018, **143**, 43; (e) G. Nagai, T. Mitsudome, K. Tsutsumi, S. Sueki, T. Ina, M. Tamm and K. Nomura, *J. Jpn. Pet. Inst.*, 2017, **60**, 256; (f) M. Ruamps, N. Lugan and V. César, *Eur. J. Inorg. Chem.*, 2017, **36**, 4167.
- 3 Y. Wang, Y. Xie, M. Y. Abraham, P. Wei, H. F. Schaefer III, P. v. R. Schleyer and G. H. Robinson, *J. Am. Chem. Soc.*, 2010, **132**, 14370.
- 4 J. B. Waters and J. M. Goicoechea, *Coord. Chem. Rev.*, 2015, **293–294**, 80; R. S. Ghadwal, *Dalton Trans.*, 2016, **45**, 16081.
- 5 (a) D. Specklin, C. Fliedel, C. Gourlaouen, J.-C. Bruyere, T. Avilés, C. Boudon, L. Ruhlmann and S. Dagorne, *Chem. – Eur. J.*, 2017, **23**, 5509; (b) A. Winkler, K. Brandhorst, M. Freytag, P. G. Jones and M. Tamm, *Organometallics*, 2016, **35**, 1160; (c) A. J. Martínez-Martínez, M. A. Fuentes, A. Hernán-Gómez, E. Hevia, A. R. Kennedy, R. E. Mulvey and C. T. O'Hara, *Angew. Chem., Int. Ed.*, 2015, **54**, 14075; (d) L. C. H. Maddock, T. Cadenbach, A. R. Kennedy, I. Borilovic, G. Aromí and E. Hevia, *Inorg. Chem.*, 2015, **54**, 9201; (e) J. B. Waters and J. M. Goicoechea, *Dalton Trans.*, 2014, **43**, 14239; (f) C. Pranckevicius and D. W. Stephan, *Chem. – Eur. J.*, 2014, **20**, 6597; (g) A. El-Hellani and V. Lavallo, *Angew. Chem., Int. Ed.*, 2014, **53**, 4489; (h) D. R. Armstrong, S. E. Baillie, V. L. Blair, N. G. Chabloz, J. Diez, J. Garcia-Alvarez, A. R. Kennedy, S. D. Robertson and E. Hevia, *Chem. Sci.*, 2013, **4**, 4259.
- 6 (a) P. K. Majhi, K. C. F. Chow, T. H. H. Hsieh, E. G. Bowes, G. Schnakenburg, P. Kennepohl, R. Streubel and D. P. Gates, *Chem. Commun.*, 2016, **52**, 998; (b) A. Winkler, M. Freytag, P. G. Jones and M. Tamm, *Z. Anorg. Allg. Chem.*, 2016, **642**, 1295; (c) M. Uzelac, A. R. Kennedy, A. Hernán-Gómez, M. A. Fuentes and E. Hevia, *Z. Anorg. Allg. Chem.*, 2016, **642**, 1241; (d) R. S. Ghadwal, S. O. Reichmann, E. Carl and R. Herbst-Irmer, *Dalton Trans.*, 2014, **43**, 13704; (e) M. Chen, Y. Wang, R. J. Gilliard Jr., P. Wei, N. A. Schwartz and G. H. Robinson, *Dalton Trans.*, 2014, **43**, 14211.
- 7 P. Ai, A. A. Danopoulos and P. Braunstein, *Inorg. Chem.*, 2015, **54**, 3722.
- 8 F. Medici, G. Gontard, E. Derat, G. Lemière and L. Fensterbank, *Organometallics*, 2018, **37**, 517.
- 9 A. Igarashi, E. L. Kolychev, M. Tamm and K. Nomura, *Organometallics*, 2016, **35**, 1778.
- 10 V. César, V. Mallardo, A. Nano, G. Dahm, N. Lugan, G. Lavigne and S. Bellemín-Laponnaz, *Chem. Commun.*, 2015, **51**, 5271.
- 11 (a) T. Freese, A.-L. Lücke, J. C. Namyslo, M. Nieger and A. Schmidt, *Eur. J. Org. Chem.*, 2018, 1646; (b) T. Freese, A.-L. Lücke, C. A. S. Schmidt, M. Polamo, M. Nieger, J. C. Namyslo and A. Schmidt, *Tetrahedron*, 2017, **73**, 5350;

(c) A.-L. Lücke, S. Wiechmann, T. Freese, Z. Guan and A. Schmidt, *Z. Naturforsch.*, 2016, **71b**, 643; (d) S. Wiechmann, T. Freese, M. H. H. Drafz, E. G. Hübner, J. C. Namyslo, M. Nieger and A. Schmidt, *Chem. Commun.*, 2014, **50**, 11822.

12 (a) G. Lavigne, V. César and N. Lugan, *Chem. – Eur. J.*, 2010, **16**, 11432; (b) V. César, N. Lugan and G. Lavigne, *J. Am. Chem. Soc.*, 2008, **130**, 11286.

13 A. Ferry, K. Schaepe, P. Tegeder, C. Richter, K. M. Chepiga, B. J. Ravoo and F. Glorius, *ACS Catal.*, 2015, **5**, 5414.

14 A. Schmidt, S. Wiechmann and C. F. Otto, *Adv. Heterocycl. Chem.*, 2016, **119**, 143.

15 A. Schmidt, S. Wiechmann and T. Freese, *ARKIVOC*, 2013, **i**, 424.

16 A. Schmidt and M. Nieger, *Heterocycles*, 1999, **51**, 2119.

17 (a) M. Liu, J. C. Namyslo, M. Nieger, M. Polamo and A. Schmidt, *Beilstein J. Org. Chem.*, 2016, **12**, 2673; (b) M. Liu, M. Nieger, E. Hübner and A. Schmidt, *Chem. – Eur. J.*, 2016, **22**, 5416.

18 J. Zhang, M. Franz, E. Hübner and A. Schmidt, *Tetrahedron*, 2016, **72**, 525.

19 N. Pidlypnyi, S. Wolf, M. Liu, K. Rissanen, M. Nieger and A. Schmidt, *Tetrahedron*, 2014, **70**, 8672.

20 C. Färber, M. Leibold, C. Bruhn, M. Maurer and U. Siemeling, *Chem. Commun.*, 2012, 227.

21 (a) C. A. Ramsden, *Tetrahedron*, 2013, **69**, 4146; (b) C. A. Ramsden and W. P. Oziminski, *Tetrahedron*, 2014, **70**, 7158; (c) W. P. Oziminski and C. A. Ramsden, *Tetrahedron*, 2015, **71**, 7191; (d) W. D. Ollis, S. P. Stanforth and C. A. Ramsden, *Tetrahedron*, 1985, **41**, 2239.

22 A. A. Granovsky, Firefly version 8, <http://www.classic.chem.msu.su/gran/firefly/index.html>.

23 M. W. Schmidt, K. K. Baldridge, J. A. Boatz, S. T. Elbert, M. S. Gordon, J. H. Jensen, S. Koseki, N. Matsunaga, K. A. Nguyen, S. Su, T. L. Windus, M. Dupuis and J. A. Montgomery, *J. Comput. Chem.*, 1993, **14**, 1347.

24 E. D. Glendening, J. K. Badenhoop, A. E. Reed, J. E. Carpenter, J. A. Bohmann, C. M. Morales and F. Weinhold, *NBO 5.9*, Theoretical Chemistry Institute, University of Wisconsin, Madison, WI, 2012.

25 G. M. Sheldrick, *Acta Crystallogr., Sect. A: Found. Crystallogr.*, 2008, **64**, 112.

26 G. M. Sheldrick, *Acta Crystallogr., Sect. C: Struct. Chem.*, 2015, **71**, 3.

